

Spatial-temporal Memories Enhanced Graph Autoencoder for Anomaly Detection in Dynamic Graphs

Jie Liu, Xuequn Shang*, Xiaolin Han, Wentao Zhang, *Member, IEEE*, Hongzhi Yin*, *Senior Member, IEEE*

Abstract—Anomaly detection in dynamic graphs presents a significant challenge due to the temporal evolution of graph structures and attributes. The conventional approaches that tackle this problem typically employ an unsupervised learning framework, capturing normality patterns with exclusive normal data during training and identifying deviations as anomalies during testing. However, these methods face critical drawbacks: they either only depend on proxy tasks for general representation without directly pinpointing normal patterns, or they neglect to differentiate between spatial and temporal normality patterns, leading to diminished efficacy in anomaly detection. To address these challenges, we introduce a novel Spatial-Temporal memories-enhanced graph autoencoder (STRIFE). Initially, STRIFE employs Graph Neural Networks (GNNs) and gated temporal convolution layers to extract spatial features and temporal features, respectively. Then STRIFE incorporates separate spatial and temporal memory networks, which capture and store prototypes of normal patterns, thereby preserving the uniqueness of spatial and temporal normality. After that, through a mutual attention mechanism, these stored patterns are then retrieved and integrated with encoded graph embeddings. Finally, the integrated features are fed into the decoder to reconstruct the graph streams which serve as the proxy task for anomaly detection. This comprehensive approach not only minimizes reconstruction errors but also refines the model by emphasizing the compactness and distinctiveness of the embeddings in relation to the nearest memory prototypes. Through extensive testing, STRIFE has demonstrated a superior capability to discern anomalies by effectively leveraging the distinct spatial and temporal dynamics of dynamic graphs, significantly outperforming existing methodologies, with an average improvement of 15.39% on AUC values.

Index Terms—Anomaly Detection, Dynamic Graphs, Graph Autoencoder, Memory Networks.

I. INTRODUCTION

Real-world networks are often modeled as dynamic graphs to reflect the changing nature of objects and their interactions [1]–[4]. In addition to basic structural details and node attributes, dynamic graphs also contain rich temporal signals, e.g., the evolving patterns of the graph structure and node attributes [5]–[7]. This temporal aspect introduces an additional

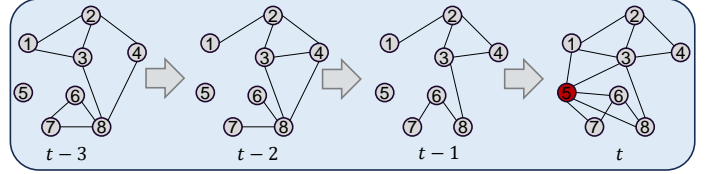


Fig. 1. A toy example of anomalies in dynamic graphs. The black nodes denote the normal nodes, and the red node denotes the abnormality, respectively. The anomaly in the graph becomes noticeable only when analyzing its temporal structural changes rather than just its spatial information from the t snapshot.

view for analyzing anomalies. For example, as shown in Fig. 1, the anomaly may not be evident when only considering the spatial information in the last graph snapshot since node 5 has similar structural information to node 3 in terms of node degrees and common neighbors. However, by observing the temporal changes in graph structures, the abnormality becomes distinctly noticeable. To avoid ambiguity, in this paper, we define the structures and attributive features within individual graph snapshots as spatial information, while characterizing the evolving changes and trends among different snapshots as temporal information. To model and integrate both the spatial and temporal signals of nodes and edges for anomaly detection, there has been a growing interest in the study of anomaly detection in dynamic graphs [8], [9].

Due to the challenge of annotating anomalous objects in real-world scenarios, anomaly detection approaches for dynamic graphs mostly employ an unsupervised learning framework [10]. The key intuition behind these methods is to develop a model that captures patterns of normality by exclusively incorporating normal data during the training phase. Subsequently, objects that the model fails to accurately represent in the testing phase are classified as anomalies. For example, AddGraph [2] employs stacked GCN and GRU to capture spatial and temporal representations of normal edges and train an edge anomaly detector with link prediction as the proxy task. Then the edges with higher prediction errors in the test set are considered abnormal. TADDY [11] encodes representation from dynamic graphs via a dynamic graph transformer in the training phase. The anomalous edges are detected based on a link prediction proxy task similar to [2] in the test phase. NetWalk [6] adopts a random-walk-based encoder to learn node representations and measures the node anomaly score by concerning its closest distance to the nor-

Jie Liu, Xuequn Shang, Xiaolin Han are with the Key Laboratory of Big Data Storage and Management, School of Computer Science, Northwestern Polytechnical University, Xi'an, Shaanxi 710129, China, Email: jayliu@mail.nwpu.edu.cn and {shang, xiaolin} @nwpu.edu.cn

Wentao Zhang is with the Center of Machine Learning Research, Peking University, Beijing 100080, China, Email: wentao.zhang@pku.edu.cn.

Hongzhi Yin is with the School of Electrical Engineering and Computer Science, the University of Queensland, St Lucia, QLD 4067, Australia, Email: h.yin1@uq.edu.au.

*Corresponding authors: Xuequn Shang and Hongzhi Yin

mal cluster centers. MTHL [12] projects multi-view dynamic graphs into a shared latent subspace and learns a compact hypersphere surrounding normal samples. Node anomalies are detected based on the distance to the learned hypersphere center. OCAN [13] seizes the normal activity patterns of observed benign users' attributes and detects fraudsters that behave significantly differently.

Despite the success of these approaches, they encounter two significant limitations: (1) Approaches such as AddGraph [2], TADDY [11], StrGNN [14], etc. only leverage proxy tasks (e.g., edge stream prediction) to derive general feature representations rather than directly identifying normal patterns. These approaches may not be effective if anomalies share commonalities, such as local structures or attributes, with normal data, especially considering the strong expressive power of representation learning models (e.g., GCN, Transformer) used in these studies. Consequently, abnormal data might also be adequately represented, resulting in suboptimal performance for anomaly detection (**P1**). (2) While methods like NetWalk [6], MTHL [12], OCAN [13], etc. explicitly model normal patterns through clustering or defining hypersphere centers, they do not distinguish the difference between spatial and temporal patterns, but instead treat them as uniform entities. However, as illustrated in Fig. 1, normal data often display distinct prototypical patterns in spatial and temporal dimensions, necessitating separate identification and storage of spatial and temporal normal patterns, respectively (**P2**).

In order to address all the limitations above, we propose a novel **S**patial-**T**emporal **m**emo**R**ies enhanced **g**ra**P**h auto**E**ncoder framework (**STR**IPE for abbreviation) for node anomaly detection in dynamic graphs. The key idea behind STRIPE is to leverage two separate memory networks [15] to identify and preserve the spatial and temporal patterns of normality and integrate them with a graph autoencoder to reconstruct graph streams as the proxy task for anomaly detection. Specifically, spatial and temporal node embeddings from input graph streams are derived using Graph Neural Networks (GNNs) and gated temporal convolution, serving as the spatial and temporal encoders, respectively. The spatial and temporal patterns are then written into their respective memory banks via a mutual attention mechanism on node embeddings, with each memory item encapsulating a prototype of normal node patterns. After that, the encoded spatial and temporal embeddings access the most closely related prototypes within the memory through mutual attention-driven retrieval. These retrieved items are subsequently merged and combined with the initial embeddings and fed into the decoder to reconstruct the graph streams.

In the training phase, spatial and temporal memory items are updated together with the encoder and decoder. We propose a comprehensive training objective that not only minimizes reconstruction errors but also reduces compactness errors which promote proximity between node embedding and its nearest memory prototype, and separateness errors which enhance the discriminative power of node embeddings to different memory items. This ensures STRIPE's effective and judicious use of the limited number of memory items, enabling the accurate extraction of normality prototypes within the training data.

In the testing phase, the learned memory items remain fixed, and the comprehensive objective now serves as the anomaly score. Since the reconstruction process integrates normality patterns preserved in memory, inputs that deviate from these prototypical patterns of normal data are likely to yield elevated anomaly scores, thereby facilitating their identification as anomalies.

In summary, the main contributions of our work are as follows:

- We propose a novel spatial-temporal memories enhanced graph autoencoder framework, STRIPE, that explicitly captures normality patterns and integrates them into graph stream reconstruction for anomaly detection. To the best of our knowledge, this is the first work to integrate memory networks for anomaly detection in dynamic graphs.
- Considering the distinct normality patterns in spatial and temporal dimensions, we develop two independent memory modules that can capture and preserve spatial and temporal patterns separately. To measure the complex relations between node embeddings and diverse spatial and temporal memory items, we propose a mutual attention mechanism to update and retrieve memory items.
- Extensive experiments have been conducted on multiple benchmark datasets, and the results of the experiment demonstrate that STRIPE achieves state-of-the-art performance with AUCs of 96.20%, 97.65%, 98.10% and 93.89% on benchmark datasets DBLP-3, DBLP-5, Reddit and Brain, respectively.

II. RELATED WORK

In this section, we introduce the works closely related to ours: Anomaly Detection in Dynamic Graphs and Memory Networks.

A. Anomaly Detection in Dynamic Graphs

Recently, the field of anomaly detection in dynamic graphs has garnered significant attention, primarily because of its capability to identify abnormalities in graphs that exhibit time-varying characteristics.

Within dynamic networks, the definition of an anomalous object varies widely depending on the specific application context. Based on the diverse nature of anomalies that can occur in such evolving structures, the scope of detection tasks can range from identifying abnormal nodes [12], [16]–[18] and edges [5], [19]–[21] to pinpointing anomalous subgraphs [22], [23]. Early approaches mainly leverage the shallow mechanisms to detect anomalies in dynamic graphs. For example, CM-sketch [5] utilizes sketch-based approximation of structural properties of the graph stream to calculate edge outlier scores. MTHL [12] distinguishes normal and anomalous nodes according to their distances to the learned hypersphere center. SpotLight [23] guarantees a large mapped distance between anomalous and normal graphs in the sketch space with a randomized sketching technique.

More recently, another branch of methods employs deep learning techniques to capture anomalous objects in dynamic

graphs [2], [6], [11], [14]. NetWalk [6] utilizes a random walk-based encoder to generate node embeddings and score the abnormality of nodes and edges with their distance to cluster centers. AddGraph [2] employs stacked GCN and GRU to capture spatial and temporal representations of normal edges and train an edge anomaly detector with edge stream prediction as the proxy task. StrGNN [14] further extracts the h-hop enclosing subgraph for each edge and employs stacked GCN and GRU to encode the extracted subgraphs for edge stream prediction. TADDY [11] learns the representations from dynamic graphs with coupled spatial-temporal patterns via a dynamic graph transformer for edge anomaly detection.

Most of the above approaches either only depend on proxy tasks for general representation without directly pinpointing normal patterns, or they neglect to differentiate between spatial and temporal normality patterns, leading to diminished efficacy in anomaly detection. STRIPE alleviates this problem by capturing distinct spatial and temporal normality patterns in the training phase and integrating the preserved normality patterns to detect anomalies in the test phase.

B. Memory Networks

To address the challenge of capturing long-term dependencies in temporal data, researchers recently proposed memory networks [15]. These networks can read and write to global memories where individual items in the memory correspond to prototypical patterns of the features. MemN2N [24] further enhances memory networks to operate in an end-to-end manner, which reduces the need for layer-wise supervision during training. Memory networks have shown effectiveness in various memorization tasks ranging from unsupervised feature learning [25], [26], one-shot learning [27], [28], to image generation [29]. Recognizing the memory's ability to capture and store prototypical patterns of normal data, more recent studies have started combining Autoencoders [30], [31] with memory modules to detect anomalies in video [32], [33] and graph [34] data.

However, the focus of these methods has largely been on video or static graph data. Our work differs by applying memory networks to dynamic graphs. We have developed distinct spatial and temporal memory modules, which allow us to analyze normal prototypes in both spatial and temporal dimensions independently.

III. PRELIMINARIES

In this section, we provide the definitions of essential concepts and formalize the problem of dynamic graph anomaly detection. We also summarize the frequently used notations across this paper in Table I for quick reference.

Definition 1: Dynamic Graph. Given a dynamic graph with overall timestamps of T , we use $\mathbb{G} = \{\mathcal{G}^t\}_{t=1}^T$ to denote the graph stream, where each $\mathcal{G}^t = \{\mathcal{V}^t, \mathcal{E}^t\}$ is the snapshot at timestamp t . \mathcal{V}^t and \mathcal{E}^t is the node set and edge set at timestamp t . An edge $e_{i,j}^t = (v_i^t, v_j^t) \in \mathcal{E}^t$ indicates the connection between node v_i^t and v_j^t at timestamp t , where $v_i^t, v_j^t \in \mathcal{V}^t$. $N^t = |\mathcal{V}^t|$ and $M^t = |\mathcal{E}^t|$ indicate the number of nodes and edges in timestamp t . The structural

TABLE I
SUMMARY OF NOTATIONS.

Notations	Descriptions
$\mathbb{G} = \{\mathcal{G}^t\}_{t=1}^T$	A graph stream with maximum timestamp of T .
$\mathcal{G}^t = \{\mathcal{V}^t, \mathcal{E}^t\}$	The graph snapshot at timestamp t .
\mathcal{V}^t	The node set at timestamp t .
\mathcal{E}^t	The edge set at timestamp t .
$v_i^t \in \mathcal{V}^t$	A node with index i at timestamp t .
$e_{i,j}^t = (v_i^t, v_j^t) \in \mathcal{E}^t$	An edge between v_i^t and v_j^t at timestamp t .
$N^t = \mathcal{V}^t $	Node number at timestamp t .
$M^t = \mathcal{E}^t $	Edge number at timestamp t .
\mathbf{A}^t	The adjacency matrix at timestamp t .
\mathbf{X}^t	The node feature matrix at timestamp t .
D	The dimension of input node features.
D'	The hidden dimension of node features.
$f(\cdot)$	anomaly detection function.
$\{\mathcal{G}^{t-\tau+1}, \dots, \mathcal{G}^t\}$	The sequence of graphs between timestamps $t - \tau + 1$ and t .
τ	Window size.
K_t	The kernel width of gated temporal convolution.
α	The balance factor for attributive and structural errors.
\mathbf{H}^t	The encoded spatial node embeddings at timestamp t .
\mathbf{Z}	The encoded temporal node embeddings for $\{\mathcal{G}^{t-\tau+1}, \dots, \mathcal{G}^t\}$.
\mathbf{M}_{sp}	spatial memory banks.
\mathbf{M}_{tp}	temporal memory banks.
\mathbf{k}_p	The key vector for memory item \mathbf{m}_p .
\mathbf{q}_i	The query vector for node i .
\mathbf{v}_i	The value vector for node i .
$\bar{\mathbf{M}}_{sp}$	The averaged spatial memory matrix.
$\bar{\mathbf{M}}_{tp}$	The averaged temporal memory matrix.
\mathbf{Z}	The decoded temporal node embeddings for $\{\mathcal{G}^{t-\tau+1}, \dots, \mathcal{G}^t\}$.
$\hat{\mathbf{H}}^{(t)}$	The decoded spatial node embeddings at timestamp t .
$\Theta_{en}^{(l)}$	The weight matrix of the l -th layer GNN in encoder.
$\Theta_{de}^{(l)}$	The weight matrix of the l -th layer GNN in decoder.
$\Phi_{en}^{(l)}$	The weight matrix of the temporal convolution kernel.
\mathbf{W}_K	The weight matrix for key vector.
\mathbf{W}_Q	The weight matrix for query vector.
\mathbf{W}_V	The weight matrix for value vector.

information of \mathcal{G}^t is represented by the graph adjacency matrix $\mathbf{A}^t \in \mathbb{R}^{N^t \times N^t}$, where $\mathbf{A}_{ij}^t = 1$ if e_{ij}^t exists, otherwise $\mathbf{A}_{ij}^t = 0$. $\mathbf{X}^t \in \mathbb{R}^{N^t \times D}$ denotes the node feature matrix at timestamp t and its i -th row vector $\mathbf{x}_i^t \in \mathbb{R}^D$ represents the feature of node v_i^t .

Definition 2: Anomaly Detection in Dynamic Graphs.

Given a dynamic graph $\mathbb{G} = \{\mathcal{G}^t\}_{t=1}^T$, our goal is to learn an anomaly detection function $f(\cdot) : \mathbb{R}^{N^t \times D} \rightarrow \mathbb{R}^{N^t \times 1}$ that can measure the degree of abnormality of the node by calculating its anomaly score $f(v_{i,j}^t)$. A larger anomaly score indicates a higher abnormal probability for $v_{i,j}^t$.

Given the challenges in obtaining and accessing anomalous labels in real-world networks, we adopt an unsupervised setting for detecting anomalies in dynamic graphs. In the training phase of this research, no node labels that indicate abnormalities are used. Instead, it is presumed that all nodes present during training exhibit normal behavior. The binary labels denoting abnormality are introduced only in the testing phase to assess the model's effectiveness. In this context, a label $y_{v_{i,j}^t} = 0$ signifies that the node $v_{i,j}^t$ is considered normal, whereas $y_{v_{i,j}^t} = 1$ identifies it as abnormal.

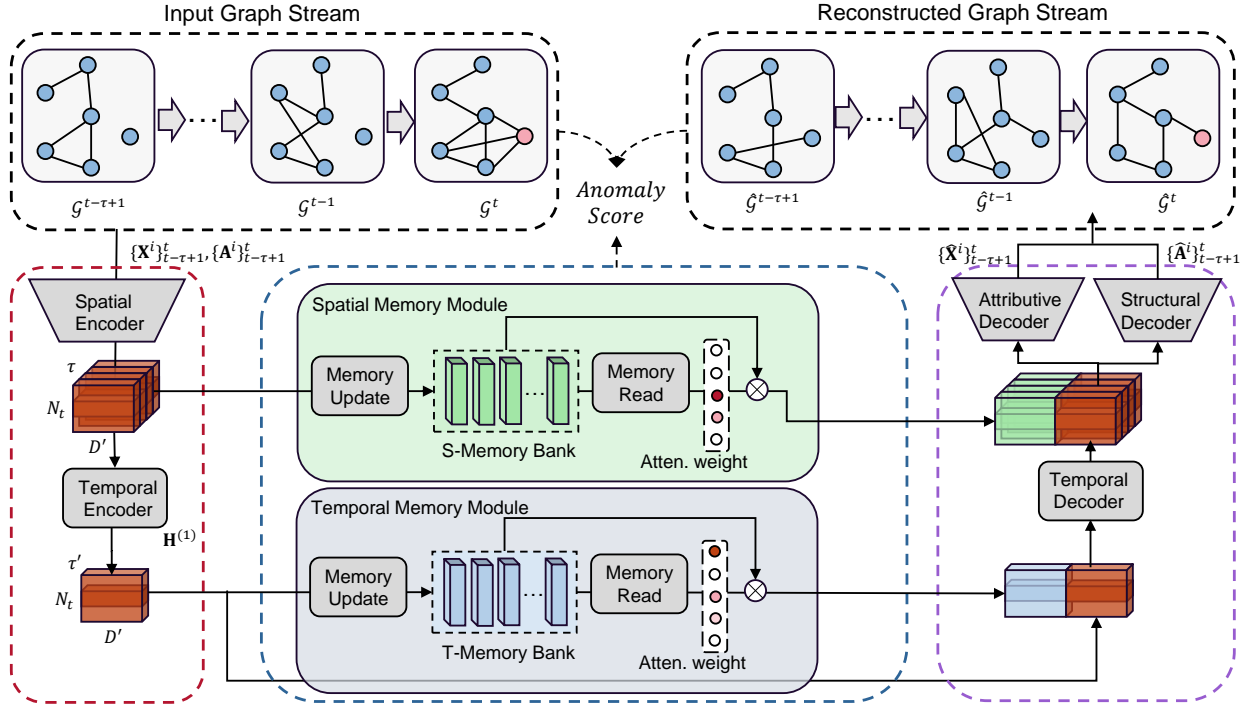


Fig. 2. Overall framework of the proposed STRIPE.

IV. METHODOLOGY

In this section, we present our proposed framework, STRIPE, designed for node anomaly detection within dynamic graphs in an unsupervised manner. As depicted in Fig. 2, STRIPE is comprised of four key components: (1) *Spatial-temporal graph encoder* that encodes both the spatial and temporal information of input graph stream into comprehensive node embeddings. (2) *Spatial-temporal memory learning* that captures and stores the prototypical patterns of normal node representations at both spatial and temporal dimensions. (3) *Spatial-temporal graph decoder* that reconstructs the original graph stream using the latent node embeddings and the identified normal prototypes, facilitating the comparison with the original input. (4) *Unified anomaly detector* that measures the abnormality of a node by calculating the reconstruction errors between the original and reconstructed graphs and the compactness errors between the node and its nearest prototype.

In the rest of this section, we introduce the four components in detail from section IV-A to V-E. The overall pipeline of STRIPE is illustrated in Algorithm (1).

A. Spatial-Temporal Graph Encoder

The input dynamic graph contains not only structural and attributive information within each graph snapshot but also abundant temporal information illustrating the evolution alongside the graph stream. Capturing both the spatial and temporal properties of dynamic graphs is essential for detecting anomalies. To address this challenge, we design a spatial-temporal encoder that consists of a spatial encoder and a temporal encoder.

1) *Spatial Encoder*: GNNs have recently emerged as one of the most powerful network representation learning approaches due to their ability to conduct deep learning on non-Euclidean graph data. In this work, we employ an L-layer GNN as the spatial encoder. Instead of inputting the whole graph stream at a time, we consider a graph sequence $\{\mathcal{G}^{t-\tau+1}, \dots, \mathcal{G}^t\}$ over a time window size τ . By adjusting the hyper-parameter τ , we can specify the receptive fields along the time axis.

The spatial encoder takes the graph sequence $\{\mathcal{G}^{t-\tau+1}, \dots, \mathcal{G}^t\}$ as input and outputs the latent node embeddings $\mathbf{H}^t \in \mathbb{R}^{N_t \times D'}$ for each snapshot \mathcal{G}^t . Specifically, node embeddings in \mathcal{G}^t are computed as follows:

$$\mathbf{H}^{(t,l)} = \text{GNN}\left(\mathbf{A}^t, \mathbf{H}^{(t,l-1)}; \boldsymbol{\Theta}_{en}^{(l)}\right), \quad (1)$$

where $\boldsymbol{\Theta}_{en}^{(l)} \in \mathbb{R}^{D \times D'}$ denotes the learnable weight parameters of the l -th layer GNN. $\mathbf{H}^{(t,l-1)}$ and $\mathbf{H}^{(t,l)}$ are the node representation matrices learned by the $(l-1)$ -th and (l) -th layer, respectively. $\mathbf{H}^{(t,0)}$ is \mathbf{X}^t . $\text{GNN}_{\theta}(\cdot)$ can be set as any off-the-shelf graph neural networks. For computation efficiency, we adopt a two-layer graph convolutional network (GCN) as the backbone. Thus, Equation (1) can be specifically re-written as:

$$\mathbf{H}^{(t,l)} = \text{ReLU}\left(\tilde{\mathbf{D}}_t^{-\frac{1}{2}} \tilde{\mathbf{A}}^t \tilde{\mathbf{D}}_t^{-\frac{1}{2}} \mathbf{H}^{(t,l-1)} \boldsymbol{\Theta}_{en}^{(l)}\right), \quad (2)$$

where $\tilde{\mathbf{A}}^t = \mathbf{A}^t + \mathbf{I}_{N_t}$, and $\tilde{\mathbf{D}}_t$ is a diagonal node degree matrix where $\tilde{\mathbf{D}}_t(i, i) = \sum_j \tilde{\mathbf{A}}^t(i, j)$. $\text{ReLU}(\cdot)$ is the activation function. We simplify $\mathbf{H}^{(t,L)}$ as \mathbf{H}^t .

2) *Gated Temporal Encoder*: Having calculated the node embeddings for each graph snapshot, we next incorporate the temporal dependencies observed across different snapshots. Prior research [2], [14] predominantly employed Recurrent

Neural Networks (RNNs) for learning temporal information. The inherent limitation of RNNs, however, is their sequential processing requirement for each time step, which significantly increases computational costs and reduces the efficiency of the model. To overcome this challenge, we utilize gated temporal convolution for temporal learning, which facilitates the parallel processing of elements within the graph sequence.

For gated temporal convolution, we employ a 1-dimensional convolution with a kernel width of K_t to capture dynamic evolving between timestamps $t - \tau + 1$ and t of the graph sequence $\{\mathcal{G}^{t-\tau+1}, \dots, \mathcal{G}^t\}$. Since the node embeddings from each snapshot influence anomaly detection differently [14], we incorporate a Gated Linear Unit (GLU) subsequent to the 1-dimensional convolution layer, which serves to accentuate critical information more significantly associated with anomaly detection.

Specifically, given $\mathbf{Z}^{(0)} = \{\mathbf{H}\}_{t-\tau+1}^t \in \mathbb{R}^{\tau \times N_t \times D'}$ as input, the gated temporal convolution is defined as follows:

$$\mathbf{Z}^{(l)} = \tanh(\mathbf{E}_1) \odot \sigma(\mathbf{E}_2), \quad (3)$$

$$\mathbf{E}_1 = \mathbf{E}^{(l-1)}[:, 1 : D'], \quad (4)$$

$$\mathbf{E}_2 = \mathbf{E}^{(l-1)}[:, D' + 1 : 2D'], \quad (5)$$

$$\mathbf{E}^{(l-1)} = \mathbf{Z}^{(l-1)} \Phi_{en}^{(l)}. \quad (6)$$

Where $\Phi_{en}^{(l)} \in \mathbb{R}^{D' \times 2D'}$ is the weight parameter of the 1-dimensional convolution kernel, \odot denotes the element-wise multiplication. $\sigma(\mathbf{E}) = \frac{1}{1+e^{-\mathbf{E}}}$ denotes the logistic sigmoid. After stacking L -layer of gated temporal convolution, the length of the graph sequence is reduced to $\tau' = \tau - L \times (K_t - 1)$. We simplify $\mathbf{Z}^{(L)} \in \mathbb{R}^{\tau' \times N_t \times D'}$ as \mathbf{Z} .

B. Spatial-Temporal Memory Learning

The spatial-temporal memory learning aims to capture and store prototypical spatial patterns and temporal patterns of normal node embeddings. Both spatial and temporal memory banks contain p memory items of dimension D' , denoted as $\mathbf{M}_{sp} \in \mathbb{R}^{P_s \times D'}$ and $\mathbf{M}_{tp} \in \mathbb{R}^{P_t \times D'}$, respectively. \mathbf{M}_{sp} and \mathbf{M}_{tp} share the same memory update and read procedures. For simplicity, we only present the learning process for \mathbf{M}_{tp} .

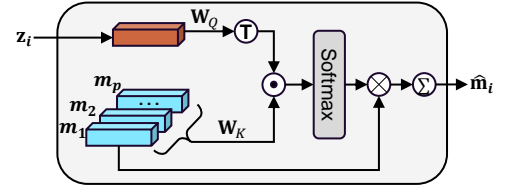
1) *Memory Read*: We denote $\mathbf{m}_p \in \mathbb{R}^{D'}$ ($p = 1, \dots, P_t$) as the item in the memory \mathbf{M}_{tp} , and $\mathbf{z}_i \in \mathbb{R}^{D'}$ ($i = 1, \dots, \tau' \times N_t$) as the item in encoded node features. As shown in Fig. 3(a), the reading process begins by calculating the attention weights between each node feature \mathbf{z}_i and all memory items \mathbf{m}_p . Prior research [34], [35] primarily adopts cosine similarity to compute self-attention, which restricts the capability to explore the relations between node features and diverse spatial and temporal memory items. To address this problem, we employ a mutual attention mechanism:

$$\mathbf{k}_p = \mathbf{m}_p \mathbf{W}_K, \quad (7)$$

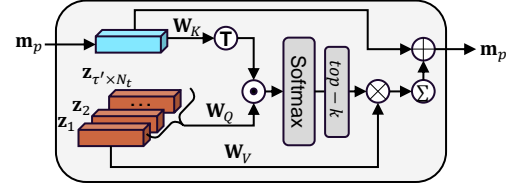
$$\mathbf{q}_i = \mathbf{z}_i \mathbf{W}_Q, \quad (8)$$

$$\mathbf{v}_i = \mathbf{z}_i \mathbf{W}_V, \quad (9)$$

where \mathbf{W}_K , \mathbf{W}_Q and $\mathbf{W}_V \in \mathbb{R}^{D' \times D'}$ are weight matrices of key vector, query vector, and value vector, respectively.



(a) memory read.



(b) memory update.

Fig. 3. The illustration of memory read and memory update procedures in the temporal memory module.

The attention weights $w_{(i,p)}$ are then computed with softmax function:

$$w_{(i,p)} = \frac{\exp(\mathbf{q}_i(\mathbf{k}_p)^T \cdot \frac{1}{\sqrt{D'}})}{\sum_{p'=1}^P \exp(\mathbf{q}_i(\mathbf{k}_{p'})^T \cdot \frac{1}{\sqrt{D'}})}. \quad (10)$$

For each node feature \mathbf{z}_i , we read the memory by a weighted average of the items \mathbf{m}_p with the corresponding weights $w_{(i,p)}$, and obtain the readout memory item $\hat{\mathbf{m}}_i^t \in \mathbb{R}^{D'}$ as follows:

$$\hat{\mathbf{m}}_i = \sum_{p=1}^P w_{(i,p)} \mathbf{m}_p, \quad (11)$$

2) *Memory Update*: During the training phase, the memory bank will also be updated to record the spatial and temporal prototypes of normal nodes. As shown in Fig. 3(b), for each memory item \mathbf{m}_p , we select the node features that are nearest to it based on the matching weights $\mu_{(i,p)}$ as follows:

$$\mu_{(i,p)} = \frac{\exp(\mathbf{q}_i(\mathbf{k}_p)^T \cdot \frac{1}{\sqrt{D'}})}{\sum_{i'=1}^{\tau' N_t} \exp(\mathbf{q}_{i'}(\mathbf{k}_p)^T \cdot \frac{1}{\sqrt{D'}})}. \quad (12)$$

Contrary to [33], [34], which utilizes all features for updating memory items, we selectively employ only the top- K relevant features. This strategy effectively filters out irrelevant, noisy nodes, thereby capturing and recording the general patterns of normal events more effectively. Therefore, the top- K values of $\mu_{(i,p)}$ are preserved, while the remainder is nullified to 0. The updated memory item \mathbf{m}_p is then calculated as follows:

$$\mathbf{m}_p \leftarrow \mathbf{m}_p + \sum_{i=1}^K \mu_{(i,p)} \mathbf{v}_i. \quad (13)$$

C. Spatial-temporal Graph Decoder

After the memory read procedure in both spatial and temporal memory modules, we obtain the averaged memory matrices $\hat{\mathbf{M}}_{tp} \in \mathbb{R}^{\tau' \times N_t \times D'}$ and $\hat{\mathbf{M}}_{sp} \in \mathbb{R}^{\tau \times N_t \times D'}$. Each item within these matrices represents the averaged spatial and temporal normal prototypes associated with the corresponding node. In

this section, we reconstruct the original graph stream with the memory matrices and the encoded latent representation \mathbf{Z} .

As shown in Fig. 2, our method inputs the concatenation of $\hat{\mathbf{M}}_{tp}$ and \mathbf{Z} into the gated temporal decoder, which is the reverse process of equation 4, and outputs $\hat{\mathbf{Z}} \in \mathbb{R}^{\tau \times N_t \times D'}$. Then we concatenate $\hat{\mathbf{M}}_{sp}$ with $\hat{\mathbf{Z}}$ and input it into the spatial decoder. We use an L-layer GCN as the attributive decoder. The l -th layer is formatted as follows:

$$\hat{\mathbf{H}}^{(t,l)} = \text{GCN}\left(\mathbf{A}^t, \hat{\mathbf{M}}_{sp}[t, :, :] \parallel \hat{\mathbf{Z}}[t, :, :]; \Theta_{de}^{(l)}\right), \quad (14)$$

where \parallel denotes concatenation operation. $\hat{\mathbf{H}}^{(t,L)}$ is $\hat{\mathbf{X}}^t$. We employ the inner product of the concatenation of $\hat{\mathbf{M}}_{sp}$ and $\hat{\mathbf{Z}}$ as the structural decoder, formatted as follows:

$$\hat{\mathbf{A}}^t = \sigma(\hat{\mathbf{M}}_{sp}[t, :, :] \parallel \hat{\mathbf{Z}}[t, :, :])((\hat{\mathbf{M}}_{sp}[t, :, :] \parallel \hat{\mathbf{Z}}[t, :, :]))^T. \quad (15)$$

Where $\sigma(\cdot)$ denotes the Sigmoid activation function.

D. Unified Anomaly Detector

In the previous sections, we have calculated the spatial and temporal prototypes and integrated them with latent representations to reconstruct the original graph stream. For a training timestamp t , the reconstruction errors can be formatted as a combination of attributive and structural reconstruction errors:

$$\mathcal{L}_{rec} = \alpha \|\hat{\mathbf{X}}^t - \mathbf{X}^t\|_2 + (1 - \alpha) \|\hat{\mathbf{A}}^t - \mathbf{A}^t\|_2, \quad (16)$$

where $\alpha \in [0, 1]$ is a hyper-parameter that balances the importance of attributive and structural errors.

Given that only normal nodes are present during the training phase, under ideal circumstances, the features of a normal node should be close to the nearest item in the memory. Conversely, the features of abnormal nodes are expected to be distant from any memory items, reflecting their deviation from normal patterns. Encouraged by this, the feature compactness loss, denoted by \mathcal{L}_{com} , is as follows:

$$\mathcal{L}_{com} = \sum_{i=1}^{\tau N_t} \|\mathbf{h}_i - \mathbf{m}_p^{sp}\|_2 + \sum_{i=1}^{\tau' N_t} \|\mathbf{z}_i - \mathbf{m}_p^{tp}\|_2, \quad (17)$$

where \mathbf{m}_p^{sp} and \mathbf{m}_p^{tp} denote the spatial and temporal memory item that is nearest to spatial embedding \mathbf{h}_i and temporal embedding \mathbf{z}_i , respectively.

Furthermore, the items within the memory should be sufficiently distant from each other. This spacing ensures that a broad spectrum of normal data patterns can be effectively captured and represented. Encouraged by this, we design the memory separateness loss, denoted as \mathcal{L}_{sep} , as follows:

$$\begin{aligned} \mathcal{L}_{sep} = & \sum_{i=1}^{\tau N_t} [\|\mathbf{h}_i - \mathbf{m}_p^{sp}\|_2 - \|\mathbf{h}_i - \mathbf{m}_n^{sp}\|_2]_+ \\ & + \sum_{i=1}^{\tau' N_t} [\|\mathbf{z}_i - \mathbf{m}_p^{tp}\|_2 - \|\mathbf{z}_i - \mathbf{m}_n^{tp}\|_2]_+, \end{aligned} \quad (18)$$

where \mathbf{m}_p^{sp} and \mathbf{m}_n^{sp} denotes the nearest and the second nearest memory item to \mathbf{h}_i . \mathbf{m}_p^{tp} and \mathbf{m}_n^{tp} denote the nearest and the

Algorithm 1: Forward propagation of STRIPE

Input: Graph stream $\{\mathcal{G}^t\}_{t=1}^T$; Number of training epochs I ; Time window size τ ; Temporal convolution kernel width K_t ; Evaluation rounds R .

Output: Anomaly scoring function $f(\cdot)$.

```

1 Randomly initialize the trainable parameters of the
  encoder, decoder, memory modules, and scoring
  function;
/* Training stage */
2 for  $i \in 1, 2, \dots, I$  do
3   for snapshot  $\mathcal{G}^t \in \{\mathcal{G}^t\}_{t=1}^T$  do
4     Calculate spatial node embeddings  $\mathbf{H}^t$  via Eq.
      (1);
5     Extract the graph sequence  $\{\mathcal{G}^{t-\tau+1}, \dots, \mathcal{G}^t\}$ ;
6     Calculate temporal node embeddings  $\mathbf{Z}$  via Eq.
      (4);
7     for  $p \in 1, 2, \dots, P$  do
8       Calculate the read attention weights  $w_{(i,p)}$ 
        via Eq. (10) and update attention weights
         $\mu_{(i,p)}$  via Eq. (12);
9     end
10    Readout the averaged memories via Eq. (11);
11    Update the memory items via Eq. (13);
12    Calculate the reconstructed attributes  $\hat{\mathbf{X}}^t$  and
      structures  $\hat{\mathbf{A}}^t$  via Eq. (14) and Eq. (15);
13    Compute the loss objective via Eq. (16), (17),
      and (18).
14  end
15 end
/* Inference Stage */
16 for  $r \in 1, 2, \dots, R$  do
17   for  $v_i \in \{\mathcal{V}^t\}_{t=1}^T$  do
18     Calculate the anomaly score for each node  $v_i$ 
      via Eq. (19).
19   end
20 end
```

second nearest memory item to \mathbf{z}_i . The total loss for training is formatted as:

$$\mathcal{L} = \mathcal{L}_{rec} + \mathcal{L}_{com} + \mathcal{L}_{sep}. \quad (19)$$

During inference, the loss in equation (19) is adopted as anomaly score. The anomaly score for each node is calculated R times to ensure that the final anomaly scores are statistically stable and reliable.

E. Complexity Analysis

In this subsection, we analyze the time complexity of each component in the STRIPE framework. We employ an L-layer GCN for spatial encoding and decoding of a graph sequence with window size τ , which brings a complexity of $\mathcal{O}(\tau L M_t D' + \tau L N_t D'^2)$, where M_t and N_t are the averaged edge and node number for each snapshot. For memory read and update, the complexity is mainly caused by mutual attention mechanism, which is $\mathcal{O}(\tau N_t^2 D')$. For gated

temporal convolution, the time complexity is $\mathcal{O}(\tau L N_t^2 D')$, which is far less than the other components and can be ignored. Therefore, to apply an L-layer STRIPE to a graph sequence of window size τ , the overall time complexity is $\mathcal{O}(\tau L (M_t D' + N_t D'^2 + N_t^2 D'))$.

V. EXPERIMENTAL STUDY

In this section, we conduct extensive experiments on four real-world benchmark datasets to evaluate the performance of STRIPE. Specifically, from section V-A to V-D, we introduce the experimental setups. Then in section V-E, we compare our method with the state-of-the-art baseline methods on the node anomaly detection task. After that, we conduct an ablation study to validate the effectiveness of each component of STRIPE in section V-F. In section V-G, we study the parameter sensitivity to further investigate the property of STRIPE. We also demonstrate the effectiveness of the proposed spatial and temporal memory modules with a case study in V-H.

A. Datasets

We assess the performance of STRIPE and its competitors on four real-world temporal networks, including two co-author networks, a social network, and a biological network. The description of the datasets is shown in Table II.

- **DBLP-3** and **DBLP-5**¹ are co-author networks where the nodes represent the authors and the edges represent the co-authorship between them. The node attributes in a network snapshot are extracted from the titles and abstracts of the corresponding author's publications during a period by word2vec. The authors in DBLP-3 and DBLP-5 are from three and five research areas, respectively.
- **Reddit**² is a social network where the nodes represent the posts. Two posts are connected if the same user comments on both posts. Two nodes are connected in a network snapshot if their corresponding posts contain similar keywords during a time period. We apply word2vec to the comments of a post to generate its node attributes
- **Brain** is a biological network, with nodes symbolizing distinct cubes of brain tissue and edges reflecting their connectivity. The network is derived from task-based functional magnetic resonance imaging (fMRI) data³ collected in real-world settings. This fMRI data is gathered while subjects perform various tasks sequentially. For each network snapshot, we utilize Principal Component Analysis (PCA) on the fMRI data of a specific time period to determine the attributes of each node. Connectivity between two nodes is established if they exhibit a similar level of activation during the observed time frame.

Due to the lack of ground-truth anomalies in these datasets, we need to manually inject synthetic anomalies into the original networks for evaluation in the testing phase. For a fair comparison, we follow the anomaly injection strategies used in [36] and [11], and inject equal numbers of structural

TABLE II
STATISTICS OF THE DATASETS. AR REPRESENTS THE ANOMALY RATIO, CALCULATED AS THE RATIO OF THE NUMBER OF ANOMALIES TO THE TOTAL NUMBER OF NODES.

Datasets	Nodes	Edges	Attributes	Timestamps	Anomalies	AR
DBLP-3	4,257	38,240	100	10	210	0.049
DBLP-5	6,606	65,915	100	10	330	0.050
Reddit	8,291	292,400	20	10	420	0.051
Brain	5,000	1,975,648	20	12	240	0.048

anomalies and attributive anomalies for each snapshot \mathcal{G}^t in the test set:

- **Structural anomaly injection.** Following [36], we generate structural anomalies by randomly selecting N_p nodes from node set \mathcal{V}^t and connecting them to form fully connected cliques. The selected N_p nodes are labeled as structural anomaly nodes. This process is repeated q times to generate q cliques. Following [36], we fix N_p as 15 and set q to 7, 11, 14, and 8 for DBLP-3, DBLP-5, Reddit, and Brain, respectively.
- **Attributive anomaly injection.** Following [11], attributive anomalies are created by randomly selecting $N_p \times q$ nodes from \mathcal{V}^t . For each chosen node v_i^t , we sample an additional k nodes to form a candidate set: $\mathcal{V}_{i,attr}^t = \{v_1^t, \dots, v_k^t\}$. Then, we replace the feature vector of v_i with the node feature from $\mathcal{V}_{i,attr}^t$ that has the largest attribute distance from v_i^t . Following [11], we set $s=2$ and $k=50$ for all the datasets.

B. Baselines

To validate the effectiveness of STRIPE, we conducted a comparative analysis with six state-of-the-art node anomaly detection baselines. This comparison includes two dynamic node anomaly detection methods: NetWalk [6] and MTHL [12]. Given the limited number of dynamic node anomaly detection baselines, we also incorporate four of the most advanced static node anomaly detection methods in our comparison: DOMINANT [36], CoLA [11], SL-GAD [37] and GRADATE [38]. Details of these baselines are introduced as follows:

Static node anomaly detection methods:

- **DOMINANT** [36] is a deep graph autoencoder-based unsupervised method that detects node anomalies by assessing the reconstruction errors of individual nodes.
- **CoLA** [11] is a contrastive learning based anomaly detection method that captures node anomaly patterns by measuring the agreement between each node and its contextual subgraph using a GNN-based encoder.
- **SL-GAD** [37] is a self-supervised anomaly detection method that combines both attribute reconstruction and contrastive learning for detecting node anomalies.
- **GRADATE** [38] is an extension of CoLA by conducting contrastive learning not only between node-node and node-subgraph pairs, but also from subgraph-subgraph pairs.

Dynamic node anomaly detection methods:

¹<https://dblp.uni-trier.de>

²<https://www.reddit.com/>

³<https://tinyurl.com/y4hwh8ro>

TABLE III

NODE ANOMALY DETECTION PERFORMANCE ON SIX BENCHMARK DATASETS, THE BEST AND SECOND TO BEST RESULTS ON EACH DATASET ARE IN BOLD AND UNDERLINED, RESPECTIVELY. PRE, F1, AND AUC REPRESENT THE PRECISION, MACRO-F1, AND AREA UNDER THE CURVE, RESPECTIVELY.

Dataset Metrics	DBLP-3			DBLP-5			Reddit			Brain		
	PRE	F1	AUC	PRE	F1	AUC	PRE	F1	AUC	PRE	F1	AUC
DOMINANT	0.1358	<u>0.5490</u>	0.6091	0.5431	<u>0.7327</u>	<u>0.9154</u>	0.4912	<u>0.6326</u>	<u>0.8717</u>	0.5845	0.5958	0.8212
CoLA	0.4753	0.4874	0.5814	0.4750	0.4872	0.4806	0.4747	0.4870	0.2410	0.4760	0.4877	0.5716
SL-GAD	0.5302	0.5193	0.6174	0.5229	0.5038	0.7638	0.4908	0.4844	0.6843	<u>0.6640</u>	0.6347	<u>0.8735</u>
GRADATE	0.5126	0.4874	0.5581	0.4923	0.4875	0.4726	0.5231	0.4870	0.5823	0.4910	0.4871	0.5629
NetWalk	0.5336	0.5092	<u>0.7126</u>	<u>0.5805</u>	0.5034	0.9107	0.5606	0.5726	0.7821	0.6239	<u>0.6643</u>	0.8590
MTHL	<u>0.5758</u>	0.5077	0.5901	0.5433	0.4951	0.7382	<u>0.6295</u>	0.6279	0.7074	0.5843	0.5988	0.8119
STRIPE	0.7622	0.7972	0.9620	0.7359	0.8020	0.9765	0.9409	0.6849	0.9810	0.6919	0.7144	0.9389

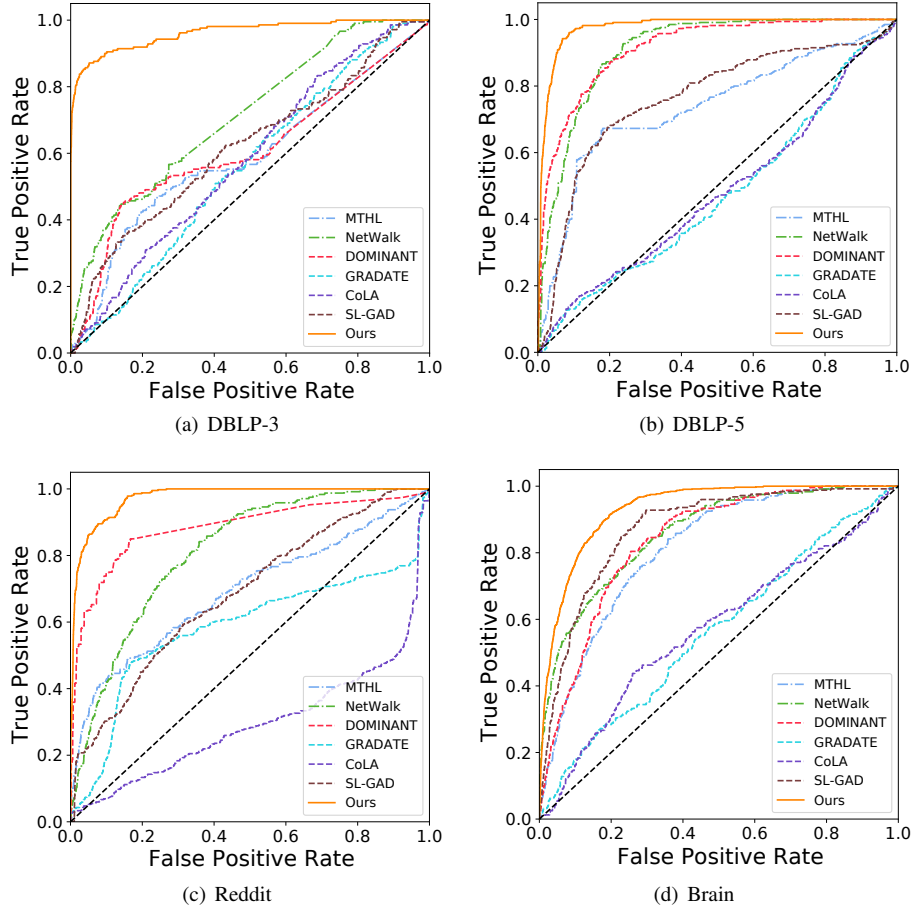


Fig. 4. ROC curves on four benchmark datasets for node anomaly detection.

- **NetWalk** [6] uses an autoencoder to update dynamic node representations and applies streaming k-means clustering for real-time node categorization. Anomaly scores are calculated based on node proximity to cluster centers.
- **MTHL** [12] learns a compact hypersphere surrounding normal node representations and then distinguishes normal and abnormal nodes according to their distances to the hypersphere center.

C. Metrics

To assess the performance of STRIPE and its competitors, we utilize a combination of ROC-AUC, precision, and Macro-

F1 as evaluation metrics. ROC-AUC, a standard metric in anomaly detection, involves plotting the true positive rate against the false positive rate, with AUC (Area Under the Curve) representing the area under this ROC curve, ranging between 0 and 1. Higher AUC values indicate better performance. Additionally, we use precision and macro-F1 as our evaluation metrics. Precision measures the proportion of positive identifications that were actually correct. Macro-F1, as the harmonic mean of precision and recall, is computed individually for each class and then averaged, to provide a balanced measure of the model's performance.

TABLE IV
QUANTITATIVE RESULTS W.R.T. PRECISION, RECALL AND AUC FOR ABLATION STUDY

Dataset Metrics	DBLP-3			DBLP-5			Reddit			Brain		
	PRE	F1	AUC	PRE	F1	AUC	PRE	F1	AUC	PRE	F1	AUC
<i>w/o attribute</i>	0.7583	0.7688	0.9513	0.7039	0.7814	0.9462	0.5042	0.5011	0.8963	0.5744	0.5478	0.7215
<i>w/o structure</i>	0.6756	0.6739	0.8351	0.6581	0.7990	0.9721	0.9344	0.6628	0.9603	0.6674	0.7046	0.9263
<i>w/o temporary</i>	0.4996	0.2371	0.5145	0.4949	0.4849	0.5547	0.6914	0.5879	0.8081	0.6919	0.6442	0.8621
<i>w/o s-prototype</i>	0.7164	0.7436	0.9491	0.7320	0.7905	0.9516	0.7897	0.7589	0.9570	0.6384	0.6802	0.8480
<i>w/o t-prototype</i>	0.6524	0.6823	0.8881	0.7248	0.7861	0.9412	0.6867	0.6487	0.9466	0.6721	0.7040	0.9022
STRIPE	0.7622	0.7972	0.9620	0.7359	0.8020	0.9765	0.9409	0.6849	0.9810	0.6919	0.7144	0.9389

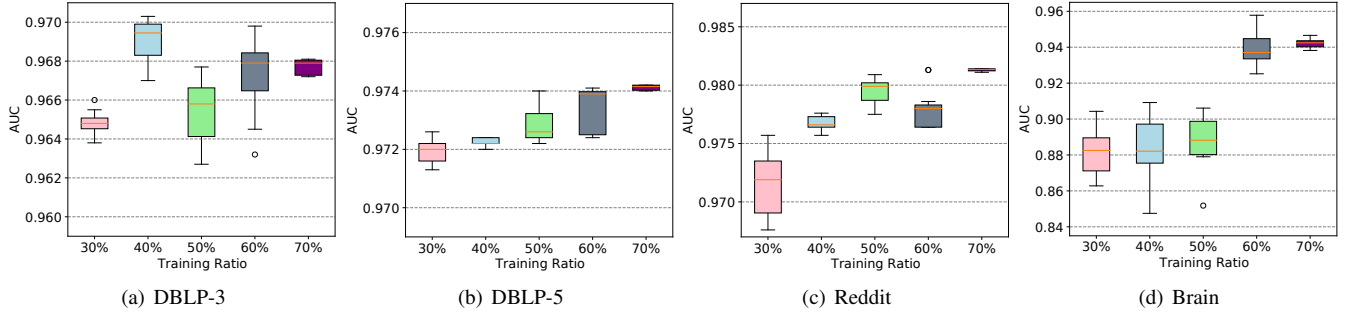


Fig. 5. AUC values of STRIPE on four datasets with different training ratios. The circular markers indicate the results which are viewed as outliers.

D. Parameter Settings

All the parameters can be tuned by 5-fold cross-validation on a rolling basis. We set the time window size τ as 3 and temporal convolution kernel width K_t as 2. Both the GCN and gated temporal convolution encoders/decoders have 2 layers with hidden dimensions set as 32 for Brain and 128 for the remaining datasets. Balance factor α is set as 0.9 for Brain and Reddit, and 0.3 for DBLP-3 and DBLP-5. The training epoch is 20 and the learning rate is 0.001 for all the datasets. Evaluation round R is 40 for Brain and 20 for the other datasets. The number of spatial and temporal memory items P_s and P_t are both set as 6. For the evaluation of static graph anomaly detection baselines, we first train these methods and measure the anomaly scores for each graph snapshot, then we derive the final score for evaluation by averaging these anomaly scores across all snapshots.

E. Comparison with the State-of-the-art Baselines

To evaluate the effectiveness of STRIPE on dynamic node anomaly detection, we compare its performance with six state-of-the-art baselines on four benchmark datasets. The precision, macro-F1 and AUC values are presented in Table III. The ROC curves can be found in Fig. 4. All the differences between our model and others are statistically significant ($p < 0.01$). According to these results, we have the following findings:

- The proposed STRIPE consistently outperforms all the baselines on the four dynamic graph datasets, showcasing its superiority in dynamic node anomaly detection. Compared with the most competitive baselines, STRIPE achieves a significant performance gain of 52.02% on precision, 25.37% on macro-F1, and 15.39% on AUC,

averagely. This validates the overall design of our proposed STRIPE model.

- Compared to static anomaly detection models (DOMINANT, CoLA, SL-GAD, and GRADATE), STRIPE integrates interactions across different timestamps through gated temporal convolution, enabling it to capture the dynamic evolution among graphs. Consequently, STRIPE learns more comprehensive embeddings for dynamic anomaly detection and achieves better performance.
- In comparison with dynamic node anomaly detection methods such as NetWalk and MTHL, STRIPE achieves 19.23% average performance gain on AUC over the best baselines. We attribute this performance advantage to our proposed prototype-enhanced reconstruction strategy. Unlike [6] and [12] that identify abnormalities based on their distances to cluster centers, our model circumvents the dependence on the selection of clustering techniques and methods for calculating distance. Instead, it directly assesses abnormalities through the reconstruction errors between the original graphs and their reconstructions, which are improved by prototypes. This eliminates potential biases introduced by specific clustering or distance computation methodologies.

F. Ablation Study

To further investigate the contribution of each component in STRIPE, we perform an ablation study in this section. The results are shown in Table IV. We set five variants of STRIPE: *w/o attribute*, *w/o structure*, *w/o temporary*, *w/o prototype* and STRIPE. Among them, *w/o attribute* excludes the attributive reconstruction error by setting $\alpha=0$. *w/o structure* excludes the structural reconstruction error by setting $\alpha=1$. *w/o tem-*

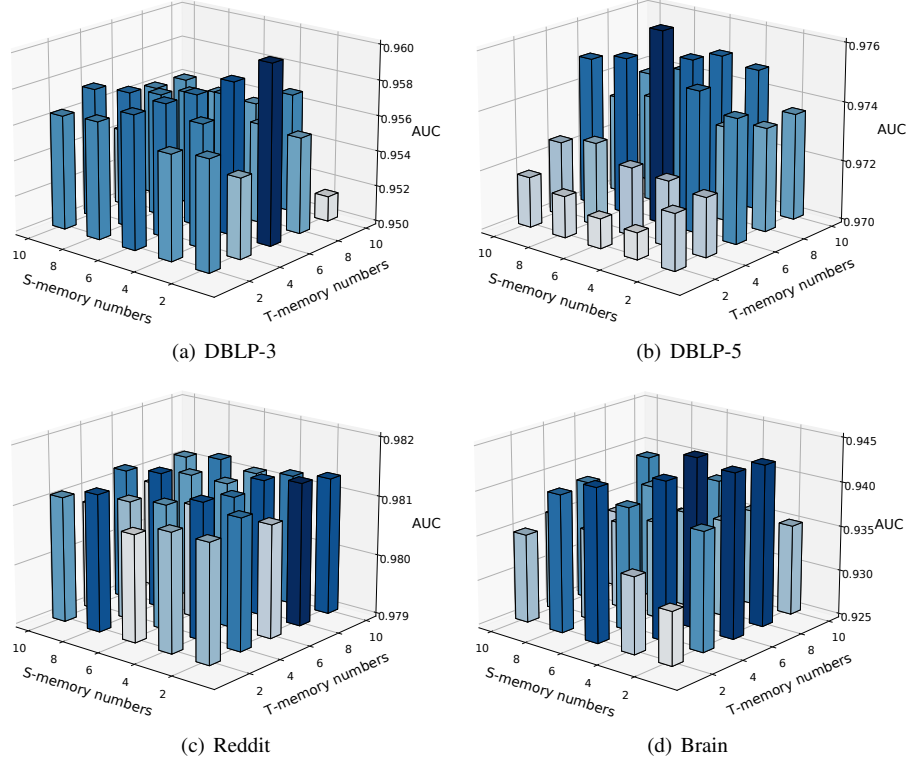


Fig. 6. The sensitivity of spatial memory item number P_s and temporal memory item number P_t on four datasets. The vertical axis represents the AUC values of STRIPE with different P_s and P_t . A darker color indicates a higher AUC value.

porary excludes the gated temporal convolution component and directly applies static version of STRIPE on each graph snapshot and computes the average anomaly scores across all the snapshots. *w/o s-prototype* and *w/o t-prototype* exclude the spatial and temporal memory modules, respectively, and reconstructs graphs without fusing prototypical patterns.

The comparison between *w/o attribute*, *w/o structure*, and STRIPE, as illustrated in Table IV, reveals a decline in performance when either attributive or structural reconstruction error is excluded from the loss function. This indicates that incorporating both types of reconstruction is essential for optimal performance in the node anomaly detection task. Furthermore, removing the gated temporal convolution component, as shown in the *w/o temporary* comparison with STRIPE, results in the most pronounced decrease in performance. This underscores the significance of tracking graph evolution for dynamic graph anomaly detection. Additionally, the performance difference between *w/o s-prototype* and STRIPE and the performance gap between *w/o t-prototype* and STRIPE further illustrate the contribution of both spatial and temporal normality memory items on the enhancement of anomaly detection performance.

G. Parameter Sensitivity

In this subsection, we conduct a series of experiments to study the impact of various hyper-parameters in STRIPE, including *training ratio*, *temporal convolution parameters*, *reconstruction weight*, *hidden dimension* and *evaluation rounds*.

1) *Training ratio*: In this experiment, we assessed the robustness of STRIPE by examining its performance across varying training ratios within the range of

{30%, 40%, 50%, 60%, 70%}. As presented in Fig. 5, the increase of training ratio results in a general improvement in AUC values across four datasets. This indicates that a larger volume of training data enhances the model’s ability to learn the normal pattern in the training set. The performance fluctuation (e.g., 40% training ratio on the DBLP-3 dataset and 60% training ratio on the Reddit dataset) is likely due to the shift in data distribution when enlarging the training set. Additionally, a decrease in AUC variance with higher training ratios suggests that STRIPE achieves more stable performance with sufficient training data. Notably, STRIPE maintains competitive performance even at a lower training ratio of 30%, demonstrating its robustness to conduct dynamic node anomaly detection from limited training data.

2) *Number of memory items*: In this research, we explore the effects of varying the number of spatial memory items (P_s) and temporal memory items (P_t) within the set {2, 4, 6, 8, 10}. The sensitivity of our model to P_s and P_t is depicted in Fig. 6. From our analysis, we derive three key insights:

The performance of our model, STRIPE, exhibits variability with adjustments in P_s and P_t across the DBLP-3, DBLP-5, and Brain datasets. Conversely, the Reddit dataset shows minimal performance fluctuation in response to changes in these parameters, likely due to its simpler normality patterns. This suggests that STRIPE can effectively capture normal spatial and temporal patterns with a minimal number of memory items, maintaining robust anomaly detection performance in simpler datasets.

For the DBLP-3, DBLP-5, and Brain datasets, we observe

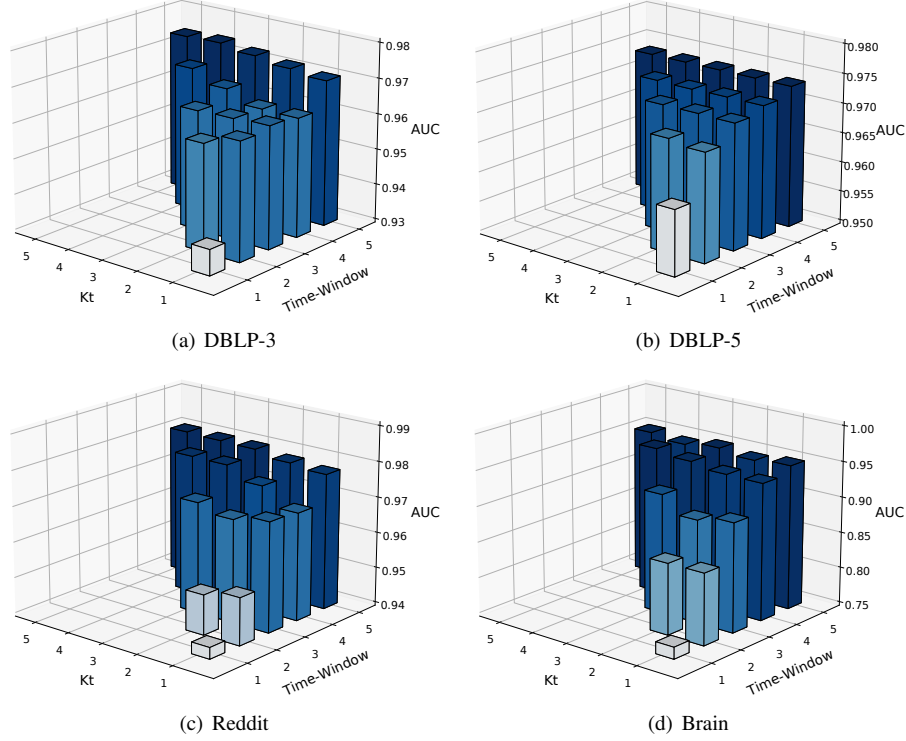


Fig. 7. The sensitivity of temporal convolution size K_t and time window size τ on four datasets. The vertical axis represents the AUC values of STRIPE with different K_t and τ . A darker color indicates a higher AUC value.

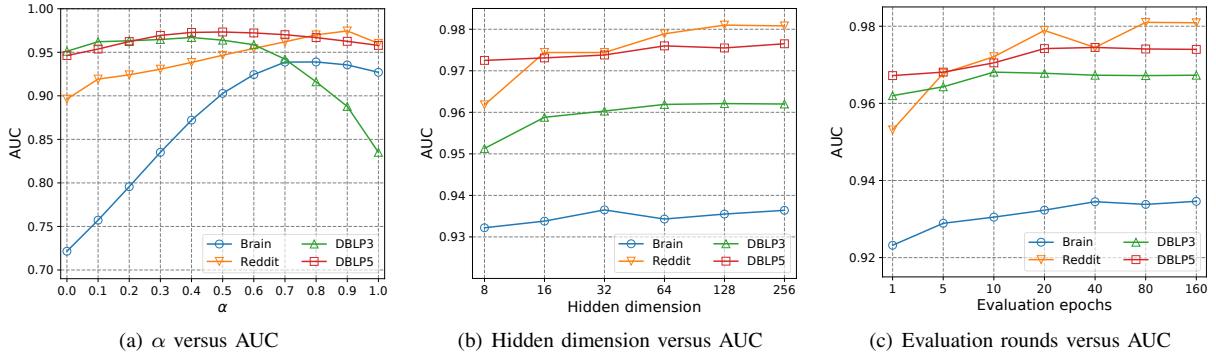


Fig. 8. AUC value of STRIPE on DBLP3, DBLP5, Reddit and Brain w.r.t. weight α , hidden dimension D' and evaluation rounds R .

that increasing P_s or P_t from lower values generally leads to higher AUC scores. For example, enhancing P_t from 2 to 6 with P_s fixed at 2 in DBLP-3 improves performance, underscoring that a sparse memory set may not adequately represent the graph's complex patterns. Nonetheless, further increasing the count of memory items beyond a certain point does not always yield better performance; it may in fact impair detection capabilities. For instance, elevating P_s from 6 to 10 while keeping P_t at 2 in Brain illustrates this trend, suggesting that excessively large memory modules might overemphasize specific details over general normality patterns, enabling abnormality to be reconstructed accurately.

The model's performance demonstrates greater sensitivity to variations in P_t compared to P_s . This indicates the temporal dimension's intricate prototypical patterns and underscores the importance of separately considering spatial and temporal

patterns for more nuanced anomaly detection.

3) *Parameters of temporal convolution:* In this study, we assess the impact of the temporal convolution kernel size (K_t) and the number of time window sizes (τ) on temporal convolution performance. We varied τ across $\{1, 2, 3, 4, 5\}$, ensuring K_t satisfies $1 \leq K_t \leq \tau$ for each value of τ . Sensitivity to changes in K_t and τ is depicted in Fig. 7.

The findings reveal suboptimal model performance when the time window size is set to 1, as temporal convolution in this scenario covers only a single graph snapshot, failing to grasp the dynamic evolution across multiple timestamps. As τ increases, we observe a notable improvement in AUC. detection performance achieves stability when $\tau \geq 4$, suggesting this time window size can adequately capture both short- and long-term dependencies in graph evolution. Further increasing τ may introduce unnecessary noise and redundancy, detracting

from the model performance.

4) *Reconstruction Weight*: In this experiment, we investigate the influence of the reconstruction weight α in Eq. (16). We vary α from 0.0 to 1.0 and analyze the corresponding AUC values. As depicted in Fig. 8(a). We can observe that for biological and social networks (Brain and Reddit), an increase in α correlates with improved AUC values, peaking at α values of 0.7 and 0.9, respectively. In contrast, for co-authorship networks (DBLP-3 and DBLP-5), optimal AUC values are observed at $\alpha \leq 0.4$, with a performance decline as α increases beyond this point. This observation suggests that the contribution of attributive and structural reconstruction error is affected by the characteristics and domains of different datasets.

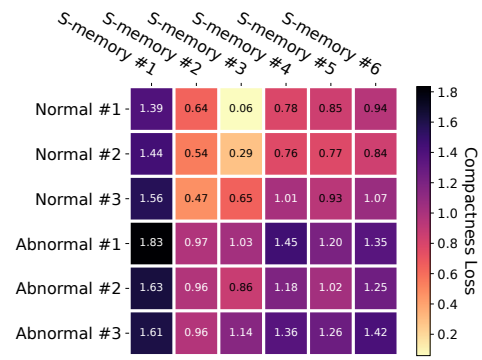
5) *Hidden Dimension*: In this experiment, we explored how varying the hidden dimension D' of both the encoder and decoder affects performance by adjusting D' from 8 to 256 and observing the AUC values. As shown in 8(b), we found that increasing D' enhances model performance within the range of [8, 128] for the DBLP-3, DBLP-5, and Reddit datasets, and within [8, 32] for Brain. Beyond these ranges, performance gains were negligible or even negative. Consequently, we opted for a D' of 32 for Brain and 128 for the other datasets.

6) *Evaluation Rounds*: In this section, we evaluated the sensitivity of STRIPE to the number of evaluation rounds (R). We adjust R from 1 to 160 to observe its impact and depict the results in Fig. 8(c). The results indicate poor detection performance at $R=1$, suggesting that a minimal number of rounds fails to adequately detect node anomalies. Performance increases for all the datasets with an increase in R . However, elevating R beyond 40 for the Brain dataset and 20 for the others does not significantly enhance results but does lead to increased computational demands. Consequently, to optimize both performance and efficiency, we establish R at 40 for the Brain dataset and 20 for the remaining datasets.

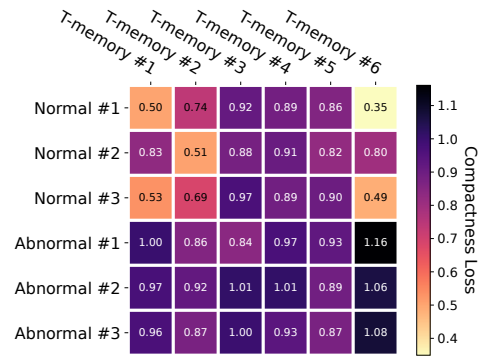
H. Case Study

In this section, we demonstrate the effectiveness of our spatial and temporal memory modules by visualizing the compactness loss between memory items with both normal and abnormal nodes. We configured the spatial and temporal memory items to six each and chose three normal and three abnormal nodes from the DBLP-3 test set for analysis. The compactness loss is calculated as outlined in Eq. 17. The findings are presented in Fig. 9, with darker colors indicating higher compactness loss and vice versa.

From Figs. 9(a) and 9(b), we note two key observations: (1) Normal nodes exhibit proximity to only a subset of memory items, showing distance from the rest. For instance, Fig. 9(a) illustrates that the compactness loss between the first normal node and the third spatial memory item is merely 0.06, considerably less than its loss with other memory items. This underscores the memory items' capacity to distinctively and effectively encapsulate normal patterns, even with a limited set of items, while ensuring sufficient separation among them. (2) Conversely, abnormal nodes display substantial compactness losses across all memory items in both spatial and temporal dimensions. As an example, the compactness losses between



(a) The compactness loss of normal and abnormal nodes w.r.t. spatial memories.



(b) The compactness loss of normal and abnormal nodes w.r.t. temporal memories.

Fig. 9. The compactness loss of normal and abnormal nodes on DBLP-3 with respect to learned spatial and temporal memory items, respectively. A darker color indicates a larger compactness loss between the node feature and the memory.

the second abnormal node and all memory items exceed 0.89, highlighting the anomaly nodes' divergence from established normal patterns. This deviation contributes to increased reconstruction errors and, consequently, elevated anomaly scores, effectively signaling their anomalous nature.

VI. CONCLUSION

In this study, we addressed the intricate challenge of anomaly detection in dynamic graphs, a domain characterized by the evolving nature of network structures and node attributes. Recognizing the limitations inherent in existing unsupervised learning frameworks, which may struggle to accurately identify anomalies due to their reliance on indirect proxy tasks or their failure to distinguish between spatial and temporal patterns, we proposed a spatial-temporal memories enhanced graph autoencoder (STRIPE) framework. STRIPE represents a novel and comprehensive approach to dynamic graph anomaly detection, distinguished by its meticulous separation and integration of spatial and temporal normality patterns. Extensive evaluation demonstrates that STRIPE significantly outperforms existing methodologies.

ACKNOWLEDGMENT

This work is partially supported by the National Key Research and Development Program of China (Grant No.

2020AAA0108504).

REFERENCES

- [1] X. Han, T. Grubenmann, R. Cheng, S. C. Wong, X. Li, and W. Sun, "Traffic incident detection: A trajectory-based approach," in *2020 IEEE 36th International Conference on Data Engineering (ICDE)*. IEEE, 2020, pp. 1866–1869.
- [2] L. Zheng, Z. Li, J. Li, Z. Li, and J. Gao, "Addgraph: Anomaly detection in dynamic graph using attention-based temporal gcN." in *IJCAI*, vol. 3, 2019, p. 7.
- [3] J. Zhang, M. Gao, J. Yu, L. Guo, J. Li, and H. Yin, "Double-scale self-supervised hypergraph learning for group recommendation," in *Proceedings of the 30th ACM international conference on information & knowledge management*, 2021, pp. 2557–2567.
- [4] B. Zheng, K. Zheng, X. Xiao, H. Su, H. Yin, X. Zhou, and G. Li, "Keyword-aware continuous knn query on road networks," in *2016 IEEE 32nd international conference on data engineering (ICDE)*. IEEE, 2016, pp. 871–882.
- [5] S. Ranshous, S. Harenberg, K. Sharma, and N. F. Samatova, "A scalable approach for outlier detection in edge streams using sketch-based approximations," in *Proceedings of the 2016 SIAM international conference on data mining*. SIAM, 2016, pp. 189–197.
- [6] W. Yu, W. Cheng, C. C. Aggarwal, K. Zhang, H. Chen, and W. Wang, "Netwalk: A flexible deep embedding approach for anomaly detection in dynamic networks," in *Proceedings of the 24th ACM SIGKDD international conference on knowledge discovery & data mining*, 2018, pp. 2672–2681.
- [7] Y. Yang, H. Yin, J. Cao, T. Chen, Q. V. H. Nguyen, X. Zhou, and L. Chen, "Time-aware dynamic graph embedding for asynchronous structural evolution," *IEEE Transactions on Knowledge and Data Engineering*, 2023.
- [8] X. Ma, J. Wu, S. Xue, J. Yang, C. Zhou, Q. Z. Sheng, H. Xiong, and L. Akoglu, "A comprehensive survey on graph anomaly detection with deep learning," *IEEE Transactions on Knowledge and Data Engineering*, 2021.
- [9] Y. Wang, J. Zhang, S. Guo, H. Yin, C. Li, and H. Chen, "Decoupling representation learning and classification for gnn-based anomaly detection," in *Proceedings of the 44th international ACM SIGIR conference on research and development in information retrieval*, 2021, pp. 1239–1248.
- [10] J. Liu, M. He, X. Shang, J. Shi, B. Cui, and H. Yin, "Bourne: Bootstrapped self-supervised learning framework for unified graph anomaly detection," *arXiv preprint arXiv:2307.15244*, 2023.
- [11] Y. Liu, Z. Li, S. Pan, C. Gong, C. Zhou, and G. Karypis, "Anomaly detection on attributed networks via contrastive self-supervised learning," *IEEE transactions on neural networks and learning systems*, vol. 33, no. 6, pp. 2378–2392, 2021.
- [12] X. Teng, Y.-R. Lin, and X. Wen, "Anomaly detection in dynamic networks using multi-view time-series hypersphere learning," in *Proceedings of the 2017 ACM on Conference on Information and Knowledge Management*, 2017, pp. 827–836.
- [13] P. Zheng, S. Yuan, X. Wu, J. Li, and A. Lu, "One-class adversarial nets for fraud detection," in *Proceedings of the AAAI Conference on Artificial Intelligence*, vol. 33, no. 01, 2019, pp. 1286–1293.
- [14] L. Cai, Z. Chen, C. Luo, J. Gui, J. Ni, D. Li, and H. Chen, "Structural temporal graph neural networks for anomaly detection in dynamic graphs," in *Proceedings of the 30th ACM international conference on Information & Knowledge Management*, 2021, pp. 3747–3756.
- [15] J. Weston, S. Chopra, and A. Bordes, "Memory networks," *arXiv preprint arXiv:1410.3916*, 2014.
- [16] T. Ji, D. Yang, and J. Gao, "Incremental local evolutionary outlier detection for dynamic social networks," in *Machine Learning and Knowledge Discovery in Databases: European Conference, ECML PKDD 2013, Prague, Czech Republic, September 23-27, 2013, Proceedings, Part II 13*. Springer, 2013, pp. 1–15.
- [17] J. Liu, L. Song, G. Wang, and X. Shang, "Meta-hgt: Metapath-aware hypergraph transformer for heterogeneous information network embedding," *Neural Networks*, vol. 157, pp. 65–76, 2023.
- [18] J. Liu, M. He, G. Wang, N. Q. V. Hung, X. Shang, and H. Yin, "Imbalanced node classification beyond homophilic assumption," *arXiv preprint arXiv:2304.14635*, 2023.
- [19] C. C. Aggarwal, Y. Zhao, and S. Y. Philip, "Outlier detection in graph streams," in *2011 IEEE 27th international conference on data engineering*, IEEE. IEEE, 2011, pp. 399–409.
- [20] K. Sricharan and K. Das, "Localizing anomalous changes in time-evolving graphs," in *Proceedings of the 2014 ACM SIGMOD international conference on Management of data*, 2014, pp. 1347–1358.
- [21] E. Manzoor, S. M. Milajerdi, and L. Akoglu, "Fast memory-efficient anomaly detection in streaming heterogeneous graphs," in *Proceedings of the 22nd ACM SIGKDD International Conference on Knowledge Discovery and Data Mining*, 2016, pp. 1035–1044.
- [22] Z. Chen, W. Hendrix, and N. F. Samatova, "Community-based anomaly detection in evolutionary networks," *Journal of Intelligent Information Systems*, vol. 39, no. 1, pp. 59–85, 2012.
- [23] D. Eswaran, C. Faloutsos, S. Guha, and N. Mishra, "Spotlight: Detecting anomalies in streaming graphs," in *Proceedings of the 24th ACM SIGKDD International Conference on Knowledge Discovery & Data Mining*, 2018, pp. 1378–1386.
- [24] S. Sukhbaatar, J. Weston, R. Fergus *et al.*, "End-to-end memory networks," *Advances in neural information processing systems*, vol. 28, 2015.
- [25] Y. Kim, M. Kim, and G. Kim, "Memorization precedes generation: Learning unsupervised gans with memory networks," in *International Conference on Learning Representations*, 2018.
- [26] Z. Wu, Y. Xiong, S. X. Yu, and D. Lin, "Unsupervised feature learning via non-parametric instance discrimination," in *Proceedings of the IEEE conference on computer vision and pattern recognition*, 2018, pp. 3733–3742.
- [27] A. Santoro, S. Bartunov, M. Botvinick, D. Wierstra, and T. Lillicrap, "Meta-learning with memory-augmented neural networks," in *International conference on machine learning*. PMLR, 2016, pp. 1842–1850.
- [28] Q. Cai, Y. Pan, T. Yao, C. Yan, and T. Mei, "Memory matching networks for one-shot image recognition," in *Proceedings of the IEEE conference on computer vision and pattern recognition*, 2018, pp. 4080–4088.
- [29] M. Zhu, P. Pan, W. Chen, and Y. Yang, "Dm-gan: Dynamic memory generative adversarial networks for text-to-image synthesis," in *Proceedings of the IEEE/CVF conference on computer vision and pattern recognition*, 2019, pp. 5802–5810.
- [30] Y. Bengio, P. Lamblin, D. Popovici, and H. Larochelle, "Greedy layer-wise training of deep networks," *Advances in neural information processing systems*, vol. 19, 2006.
- [31] T. N. Kipf and M. Welling, "Variational graph auto-encoders," *arXiv preprint arXiv:1611.07308*, 2016.
- [32] D. Gong, L. Liu, V. Le, B. Saha, M. R. Mansour, S. Venkatesh, and A. v. d. Hengel, "Memorizing normality to detect anomaly: Memory-augmented deep autoencoder for unsupervised anomaly detection," in *Proceedings of the IEEE/CVF International Conference on Computer Vision*, 2019, pp. 1705–1714.
- [33] H. Park, J. Noh, and B. Ham, "Learning memory-guided normality for anomaly detection," in *Proceedings of the IEEE/CVF conference on computer vision and pattern recognition*, 2020, pp. 14 372–14 381.
- [34] C. Niu, G. Pang, and L. Chen, "Graph-level anomaly detection via hierarchical memory networks," in *Joint European Conference on Machine Learning and Knowledge Discovery in Databases*. Springer, 2023, pp. 201–218.
- [35] Y. Liu, J. Liu, M. Zhao, D. Yang, X. Zhu, and L. Song, "Learning appearance-motion normality for video anomaly detection," in *2022 IEEE International Conference on Multimedia and Expo (ICME)*. IEEE, 2022, pp. 1–6.
- [36] K. Ding, J. Li, R. Bhanushali, and H. Liu, "Deep anomaly detection on attributed networks," in *Proceedings of the 2019 SIAM International Conference on Data Mining*. SIAM, 2019, pp. 594–602.
- [37] Y. Zheng, M. Jin, Y. Liu, L. Chi, K. T. Phan, and Y.-P. P. Chen, "Generative and contrastive self-supervised learning for graph anomaly detection," *IEEE Transactions on Knowledge and Data Engineering*, 2021.
- [38] J. Duan, S. Wang, P. Zhang, E. Zhu, J. Hu, H. Jin, Y. Liu, and Z. Dong, "Graph anomaly detection via multi-scale contrastive learning networks with augmented view," in *Proceedings of the AAAI Conference on Artificial Intelligence*, vol. 37, no. 6, 2023, pp. 7459–7467.



Jie Liu received his BS degree from Northwestern Polytechnical University, Xi'an, China in 2019. He is currently pursuing a Ph.D. degree in computer science at Northwestern Polytechnical University, Xi'an China. His research interests range from data mining, graph neural networks, and graph anomaly detection. He has published 5 papers in the areas of graph representation learning and graph anomaly detection in top-tier conferences and journals (e.g., IJCAI, ICDE, AAAI).



Xuequn Shang received her Ph.D. degree in German in 2005. She is currently a professor and serves as the Dean of the School of Computer Science at Northwestern Polytechnical University. Her research interests include data mining, machine learning, big data, and bioinformatics. She has published over 100 papers in prestigious academic journals and authoritative international conferences such as Nature Communications, Cell Reports, Briefings in Bioinformatics, Bioinformatics, IJCV, TMM, ICDE, IJCAI, and AAAI.



Xiaolin Han received her PhD degree from the Department of Computer Science at the University of Hong Kong (HKU) in 2022. Xiaolin Han joined Northwestern Polytechnical University (NWP) in November of 2022 as an associate professor at MIT Key Laboratory of big data storage and management. Her research interests include spatial-temporal data mining, trajectory outlier detection, and traffic incident detection. Till now, Xiaolin Han has published 10 papers in the areas of data mining and database, and most of them were published in top-tier conferences and journals (e.g., PVLDB, ICDE, and SIGMOD).



Wentao Zhang received his PhD degree in computer science at Peking University (PKU) in 2020. He is an assistant professor in the Center of Machine Learning Research at PKU, and he leads the Data-centric Machine Learning (DCML) group. His research focuses on DCML, graph machine learning, machine learning systems and AI4Science. He has published 40+ papers, including 10+ first-author papers in the top DB (SIGMOD, VLDB, ICDE), DM (KDD, WWW), and ML (ICML, NeurIPS, ICLR) venues.



Hongzhi Yin received a PhD degree in computer science from Peking University, in 2014. He works as an ARC Future Fellow and Full Professor at The University of Queensland, Australia. He has made notable contributions to recommendation systems, graph learning, and decentralized and edge intelligence. He has published 300+ papers with an H-index of 70 and received the prestigious IEEE Computer Society's AI's 10 to Watch Award, AIPS Young Tall Poppy Science Award, ARC Future Fellowship 2021 and DECRA Award 2016.